RAL-90-098

Science and Engineering Research Council
Rutherford Appleton Laboratory
Chilton DIDCOT Oxon OX11 0QX

RAL-90-098

Muonium Substituted Molecules.

SFJ Cox

December 1990

Science and Engineering Research Council

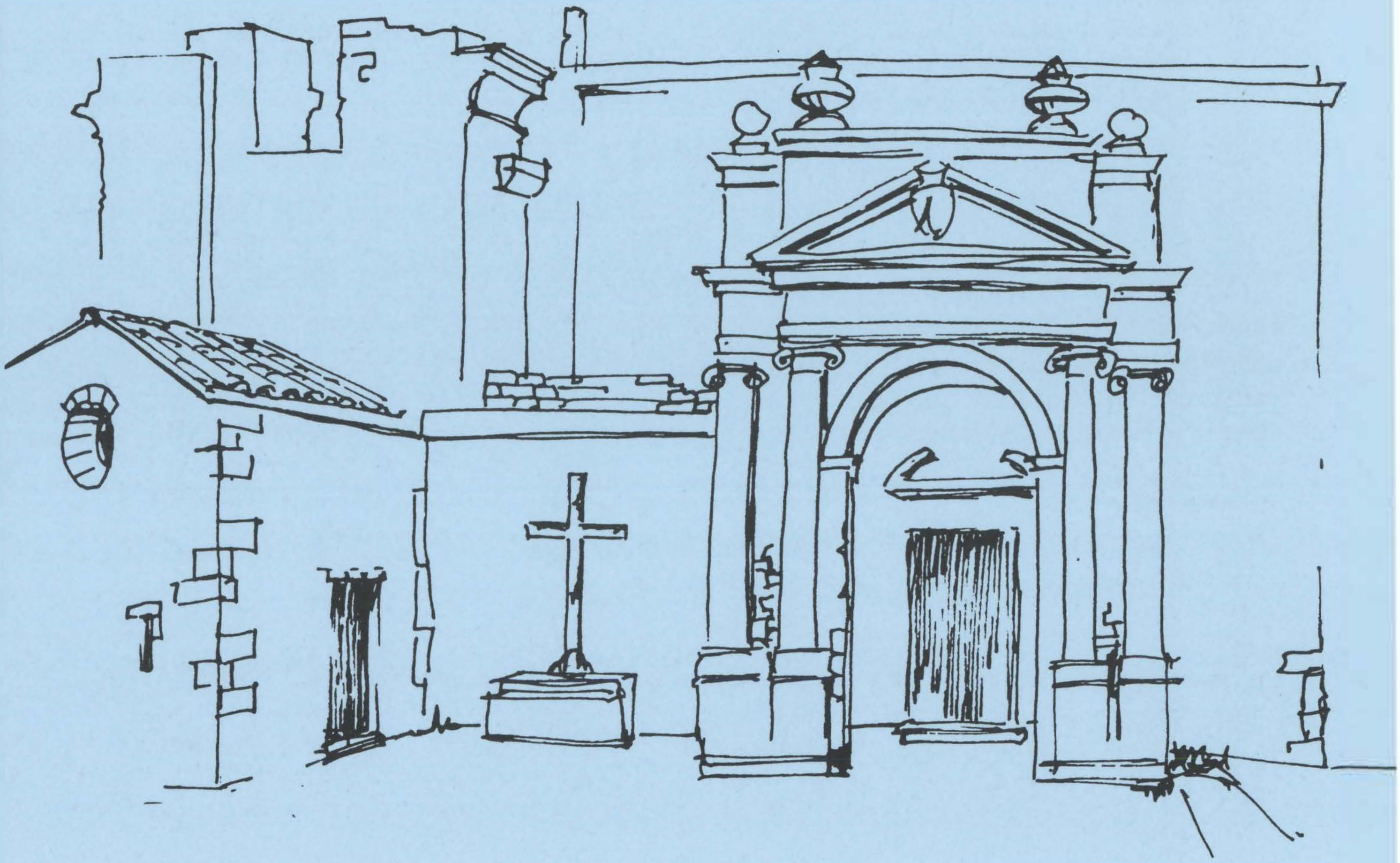

San Domenico
E Majorana centre

MUONIUM SUBSTITUTED MOLECULES

SFJ Cox
ISIS Pulsed Muon Facility
Rutherford Appleton Laboratory
Chilton, Oxfordshire, OX11 0QX, UK

Lecture given at the International Workshop on Exotic Atoms in Condensed Matter, Erice, Sicily (19-25 May 1990)

ABSTRACT

The manner in which Muon Spin Rotation and Level Crossing Resonance are used to characterise muonium substituted organic radicals is described, and illustrated with spectra for the ethyl radical and related species. Comparison with ESR data for the unsubstituted radicals reveals significant structural and hyperfine isotope effects which can be traced to the effects of zero point motion. The first comparable results for a diamagnetic species, exhibiting a quadrupole isotope effect by comparison with conventional NQR data, are presented and discussed.

1. ANALOGIES

Implanted in matter, whether in the solid, liquid or gas phase, positive muons cannot remain as free particles. They seek to lower their energy by the acquisition of electrons. In metals they attract a screening charge of conduction electrons. In gases they stick to atoms (even rare gas atoms) or molecules to form molecular cations or else they strip electrons from the host atoms to form the hydrogen-like atom, μ^+e^-, called muonium. In solids which are insulating or semiconducting, muonium can also be formed, though its properties are modified significantly from those of the free atom; in fact, the stable state may be thought of as the result of a chemical reaction with the host. Likewise in molecular materials, including organic liquids, muonium can be formed - and subsequently react chemically.

In this "chemical" behaviour, the positive muon resembles the proton. Whereas the negative muon plays the role of a heavy electron the positive muon does not play the role of a heavy positron! It adopts localised rather than propagating states in crystalline lattices; it adopts the position of an atomic nucleus rather than an "orbital" state in molecules. It is even worth mentioning that it is used experimentally to probe spin density (compare proton NMR) rather than charge density (contrast positron annihilation) and that its lifetime is unaffected by its chemical state or environment.

Likening the positive muon to a proton would horrify nuclear or high energy physicists! The point is that as far as solid state and chemical physics are concerned, where the phenomena of interest are characterised by energies $\lesssim$ 10 eV, the fact that the muon does not experience the Strong Interaction is usually unimportant. Chemical behaviour is determined by the electromagnetic interaction. The fact that the muon decays via the Weak Interaction is the basis of μSR spectroscopy!

2. NOMENCLATURE

Muonium is an unfortunate name, which should have been reserved for $\mu^+\mu^-$. However, we are stuck with it. The muonium - protium analogy can be further underlined by the contrast with positronium, $Ps = e^+e^-$, which has no central nucleus and only half the binding energy of the hydrogen isotopes. Since the electron in muonium has a reduced mass only 0.5% smaller than in protium, muonium in fact has a size and binding energy very similar to that of hydrogen. Whether it can formally be called a light isotope of hydrogen is perhaps a pedantic question; certainly this is how it behaves chemically /1/. The nomenclature Mu has been adopted both to denote the atomic state and as the chemical symbol. In the following, Mu^+ is used for any cationic species in which the positive muon is associated with a molecule or cluster; μ^+ is reserved for the energetic free particle.

Much of this Lecture is concerned with muonium which is covalently bonded in organic radicals. These paramagnetic molecules are particularly amenable to study. They are often formed when positive muons are implanted in (unsaturated) organic compounds. They display characteristic frequencies in the muon spin rotation spectra from which the muon-electron hyperfine coupling can be measured and the radical itself identified. That is, the position adopted by muonium in the molecule can be determined. These molecules are called "muonium substituted" in the sense that they each have counterparts in which hydrogen occupies this position, the great majority known previously to conventional radical chemistry and ESR spectroscopy. Thus the ethyl radical $\dot{C}H_2.CH_3$ has a muonium substituted version $\dot{C}H_2.CH_2Mu$. The muon hyperfine couplings are expected to be governed by the same factors as the proton hyperfine constants in "ordinary" radicals and so may be interpreted in the same manner in terms of the electronic and conformational structure of these molecules.

3. DYNAMICAL ISOTOPE EFFECTS

In this respect, muonium substitution may be compared with the more familiar process of deuteration. Of interest is the effect of isotopic substitution on the various 1-electron molecular properties. Deuteration rarely causes these properties to change by more than a few percent, however. The effects are greatly enhanced by muonium substitution, by virtue of the much higher isotopic mass ratio, $m_\mu / m_p \simeq 1/9$. Such a ratio has been described as "unprecedented in the chemical literature" /2/.

Especially it is the existence of a light isotope of hydrogen which gives this enhancement, and favours the observation of quantum dynamical effects. Hyperfine couplings are arguably the easiest 1-electron property to measure with precision and in μSR studies of molecular species they have to date received almost exclusive attention. Hyperfine isotopic effects are displayed by a comparison of μSR data on the muonium substituted radicals with ESR data on their unsubstituted counterparts. This is the subject of Sections 4-14.

The first measurement of a quadrupole isotope effect is reported in Sections 15-16, where the prospects for future studies in this and other areas are also examined.

4. ESR AND μSR SPECTROSCOPY

The different manner in which hyperfine couplings are measured by ESR and μSR is illustrated in Figure 1. ESR makes use of transitions of the electron spin, which are shown as light arrows. These are detected at constant frequency and the proton hyperfine constant deduced from the separation of the resonant fields. μSR makes use of the transitions shown as bold arrows; these are analogous to ENDOR transitions in conventional magnetic resonance.

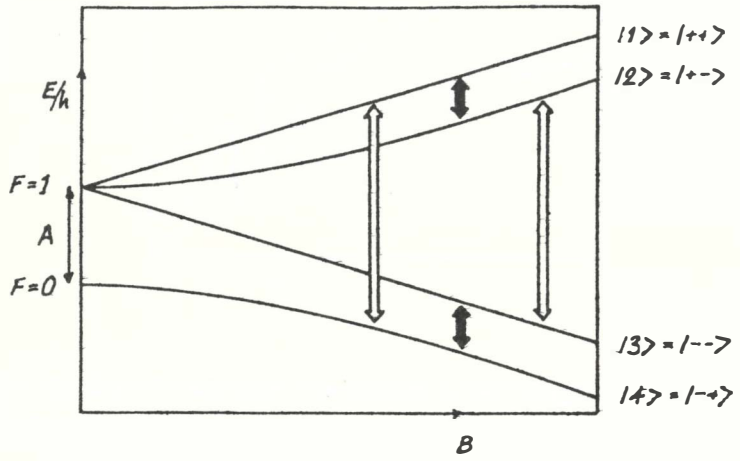

Figure 1. Breit-Rabi diagram for one electron spin (S = ½) and one nuclear spin (I = ½) with an isotropic hyperfine coupling **AI.S**. Light arrows indicate the ESR transitions and bold arrows the μSR or ENDOR transitions.

Figure 1 is the Breit-Rabi diagram. This was originally conceived for atomic hydrogen but serves equally well for muonium. It also serves for muonium-substituted radicals - provided the muon-electron hyperfine coupling is isotropic and the hyperfine couplings to other nuclei can be neglected. This is surprisingly often the case! Anisotropy of the couplings is not detected in the liquid (or gas) phase, since it is averaged out by the rapid tumbling motion of the molecules. Muon (or proton) hyperfine couplings in organic radicals rarely exceed 10% of their value in free muonium (or hydrogen) so the Paschen-Back regime is reached in correspondingly lower fields - typically a few kilogauss /3/. When all the nuclear spins present are decoupled, the μSR spectrum collapses to two lines, as illustrated in Figure 2. (The complexity of the ESR spectrum, as more nuclei are "added", can readily be imagined). The muon hyperfine coupling constant A_μ is given (exactly) by the sum of the frequencies of the two transitions - or their difference, according as $A_\mu/2$ is greater or less than the muon Larmor frequency in the applied magnetic field:

$$A_\mu = \nu_{12} \pm \nu_{34} \qquad (A_\mu/2 \gtrless \tfrac{1}{2\pi}\gamma_\mu B).$$

5. ESR SPECTRUM OF THE ETHYL RADICAL

The ethyl radical and its muonium substituted counterpart have been exhaustively studied by ESR and μSR respectively and are almost understood! As prototype or parent of all the alkyl radicals they serve as a good example of how the various hyperfine couplings are measured and interpreted.

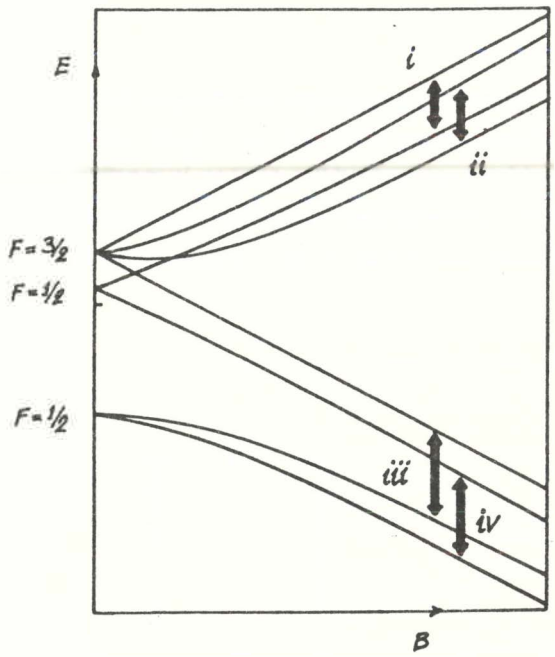

Figure 2. Zeeman diagram for a radical with isotropic couplings between the electron and two spin-½ nuclei. The transition frequencies (i) and (ii) become equal in high field, as do (iii) and (iv).

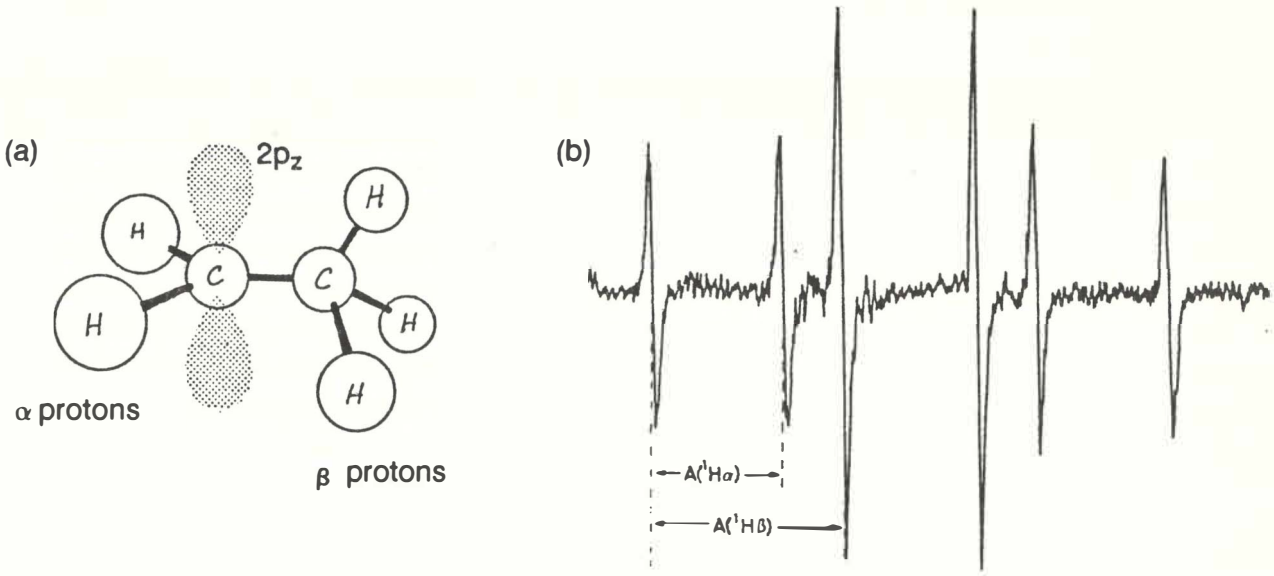

Figure 3. Structure (a) and ESR spectrum (b) (recorded in the liquid phase /4/) of the ethyl radical.

The unsubstituted radical $\dot{C}H_2CH_3$ and its ESR spectrum are illustrated in Figure 3. Major spin density is located on the trigonal carbon atom and is depicted in 3(a) as localised in an atomic $2p_z$ orbital. Actually, the singly occupied molecular orbital (the SOMO) spreads over the whole molecule. The methylene or α protons lie on a nodal plane of this orbital, so their couplings are due to spin polarisation and are expected to be negative. The corresponding splittings may be seen in 3(b)), although their sign cannot in fact be determined from the simple ESR spectrum.

Admixture of the methyl group C-H bonding orbitals in the SOMO amounts to a leakage of spin density onto the β protons. Their hyperfine coupling must therefore be positive; it corresponds to the larger splitting in 3(b). The delocalisation is known as hyperconjugation. The equivalence of the three β protons indicates that the methyl group is free to rotate about the C-C bond (at all temperatures).

6. FORMATION OF THE RADICALS

The ethyl radical is formed by γ-irradiation of ethene under the correct conditions - a hydrogen atom is removed radiolytically from one molecule and reacts by addition with another, breaking the carbon-carbon double bond /4/ (here the dot is used to emphasise the presence and position of the unpaired electron spin):

$$CH_2=CH_2 + H\cdot \rightarrow \dot{C}H_2\text{-}CH_3$$

Its muonium substituted counterpart is formed by muon-irradiation of ethene.The possible processes involved following muon implantation (in organic liquids) are considered elsewhere /5/. Formally at least, the net result corresponds to the addition of muonium in an analogous fashion:

$$CH_2=CH_2 + Mu\cdot \rightarrow \dot{C}H_2CH_2Mu.$$

7. μSR SPECTRUM OF THE SUBSTITUTED RADICAL

A μSR spectrum for $\dot{C}H_2CH_2Mu$, showing the two characteristic "high field" lines (plus a third from muons reaching a diamagnetic state) is given in Figure 4. Only the muon hyperfine coupling can be deduced from such a spectrum. Fortunately another technique exists to

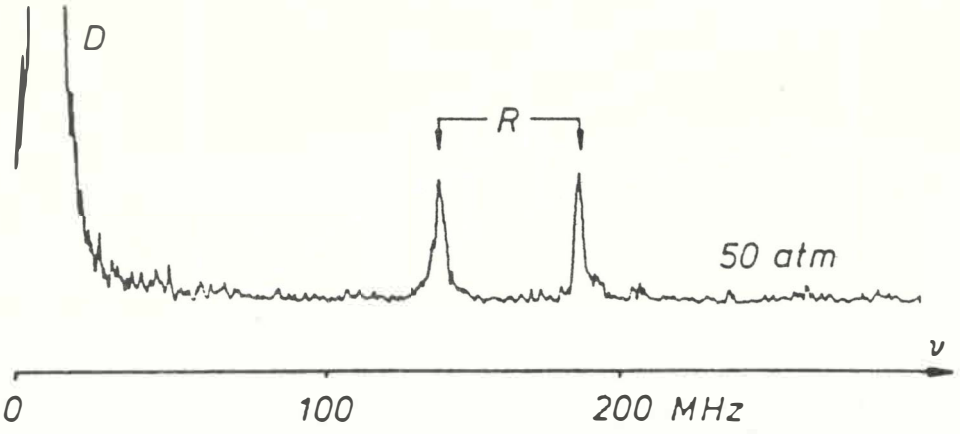

Figure 4. μSR spectrum of the muonium substituted ethyl radical, $\dot{C}H_2CH_2Mu$, in gaseous ethene at 50atm (from Roduner and Garner /7/.) Such spectra are still visible with good signal to noise ratio down to 1atm pressure /8/!

determine the other couplings - including their sign (Section 8). This is just one example of the large number of muonium substituted radicals which have now been identified /3/ - over 300 to date /6/. The majority have been studied in the liquid phase.

The remarkable feature of this spectrum is that it was detected in the gas phase! To put this achievement in context, no ESR spectrum has been reported for the ordinary ethyl radical (or for any other of such high molecular weight) in the gas phase. Coupling to total angular momentum splits gas phase ESR spectra into a multitude of lines corresponding to different rotational states so that they become impossible to detect except for diatomic and a few triatomic species.

8. LEVEL CROSSING RESONANCE

Of the two frequencies displayed in a high field μSR spectrum, one corresponds to the hyperfine field at the muon adding to the applied magnetic field, the other to it subtracting. The same is true for ENDOR-type transitions of other nuclear spins. It is therefore always possible to tune the applied field so that the transition frequencies of the muon and another nucleus exactly match. This puts the muon and the other nucleus "on speaking terms" so that they may exchange polarisation by cross-relaxation.

This is the principle of the technique known as Level Crossing Resonance /9/ as applied to paramagnetic species /10/. Purists refer to it as Avoided Level Crossing /11/ since the cross relaxation can only occur, of course, if the degeneracy of the crossing is lifted - as illustrated in the insert to Figure 5.

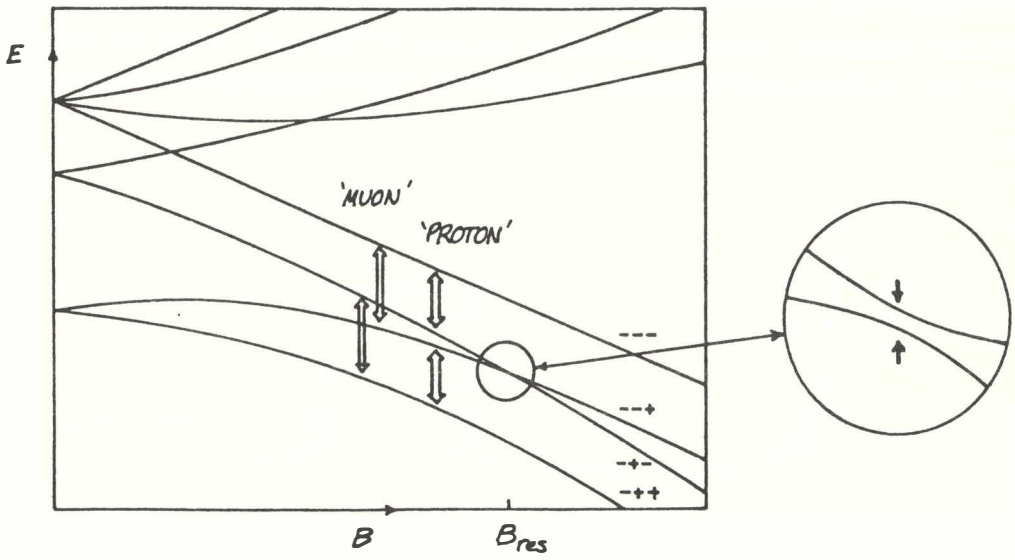

Figure 5. Level crossing and its "avoidance". The energy level diagram of Figure 2 is redrawn to show the resonant coincidence of muon and proton transition frequencies. The resonance condition can always be met - if the sign of the proton coupling is reversed the level crossing occurs in the upper group of levels instead! The splitting shown in the insert is a measure of the cross relaxation or polarisation transfer rate.

A spectrum for the muonium substituted ethyl radical is given in Figure 6. Knowing the muon hyperfine coupling A_μ (from data such as that in Figure 4), the α and β proton couplings in $\dot{C}H_2CH_2Mu$ can be determined with great precision from the position of the two resonances. For each set of equivalent nuclei the condition is of the form /10,11/

$$B_{res} = \pi[(A_\mu - A_n)/(\gamma_\mu - \gamma_n) - (A_\mu + A_n)/\gamma_e]$$

$$\simeq \pi(A_\mu - A_n)/(\gamma_\mu - \gamma_n)$$

so that even the relative signs of the couplings are available. Again, most work to date has been on liquid samples, but Figure 6 is a gas-phase spectrum chosen as an example of recent developments, and to show that Level Crossing Resonance is equally powerful in the gas phase. (In fact, it is easier than ordinary μSR - the requirement on radical formation rate is less stringent).

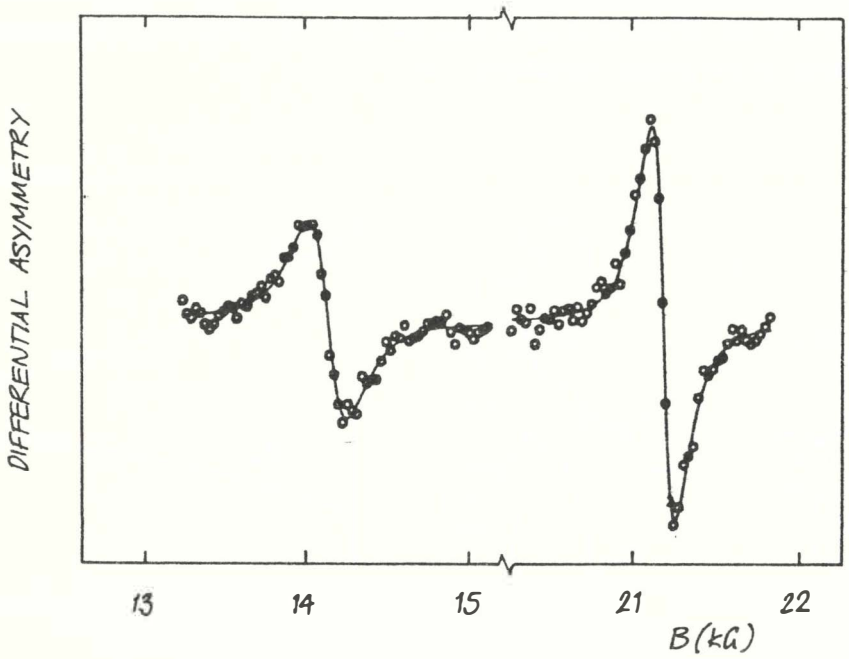

Figure 6. LCR spectrum of CH_2CH_2Mu in ethene gas at 6.5atm (from /8,13/).

The combination of (transverse field) μSR and (longitudinal field) LCR is therefore able to give a complete characterisation of the muonium substituted radicals. It could even be said to better ESR in giving the signs of the couplings and extending measurements to the gas phase!

9. THE HYPERFINE ISOTOPE EFFECT

In order to compare the muon and proton hyperfine couplings, determined from such spectra, it is customary to scale down the muon value by the ratio of the particles' magnetic moments, and use the "reduced" value:

$$A'_\mu = (\mu_p/\mu_\mu)A_\mu = 0.314A_\mu$$

It has been known for some time that the reduced muon coupling in the ethyl radical, as in the other alkyl radicals, is greater than the normal proton coupling /3/. This indicates that the substituted group CH_2Mu is not free to rotate like the ordinary methyl group but adopts instead a preferred orientation, maximising overlap or hyperconjugation of the C-Mu bonding orbital with the unpaired electron wavefunction (Figure 7a). The temperature dependence of A_μ allows the effective barrier to rotation to be determined/12/.

The LCR data (A_p in Figure 7b) confirm this behaviour. When the muon effectively eclipses the $2p_z$ orbital (giving a high value of A_μ) the two protons are held near the nodal plane (giving a low value of A_p). Torsional oscillation becomes important as the temperature is raised and, as free rotation is approached, spin density on the muon becomes more nearly equal to that on the CH_2Mu protons.

Recent data shows the curves of Figure 7(b) extending smoothly through the freezing and boiling points. There is no significant change to the internal (intramolecular) barrier to rotation in $\dot{C}H_2$-CH Mu, therefore, at the phase transitions /13/.

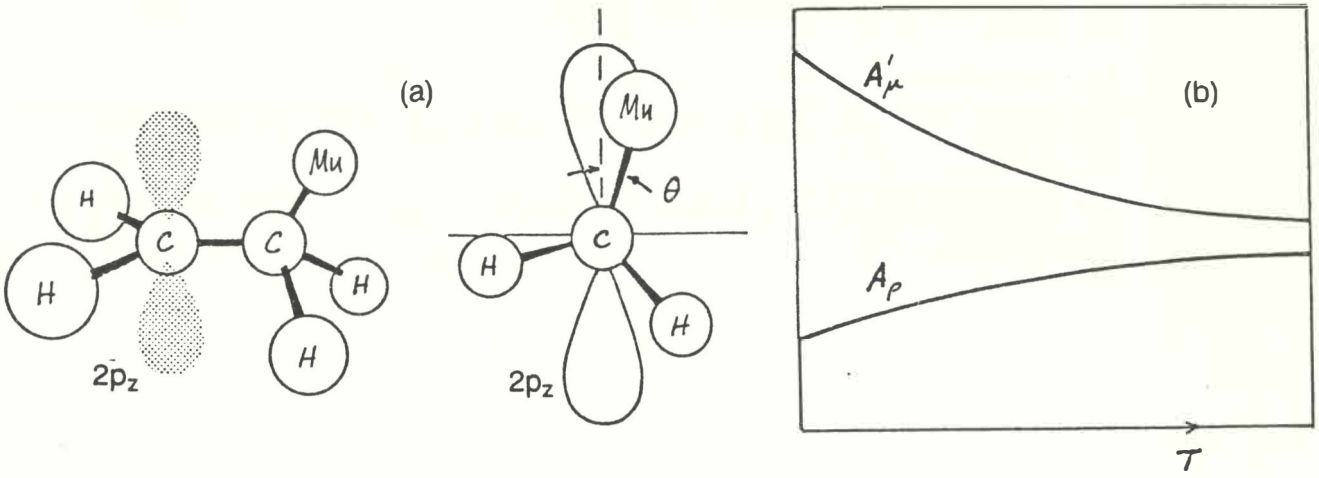

Figure 7. Structure of the substituted ethyl radical $\dot{C}H_2CH_2Mu$, including an end-on view illustrating the 'eclipse' of the $2p_z$ orbital by the C-Mu σ-bond (a). As temperature increases the amplitude of thermal libration about $\theta = 0$ increases, resulting in variation of the β couplings sketched qualitatively in (b).

10. THE TERTIARY-BUTYL RADICAL: LIQUID AND SOLID PHASE DATA

A nice illustration of the same effect is given by liquid phase data for the tertiary butyl radical. (This species can be considered derived from the ethyl radical by replacing the two α protons with methyl groups, to give a more symmetric molecule: Figure 8a). LCR spectra are shown in Figure 8(b). The stronger resonance is from protons in the CH_3 groups (which rotate freely at all temperatures); the weaker is from protons in CH_2Mu groups. The resonances move closer together with increasing temperature, as free rotation of the CH_2Mu group is approached. (The overall shift of both resonances reflects the variation of the muon coupling).

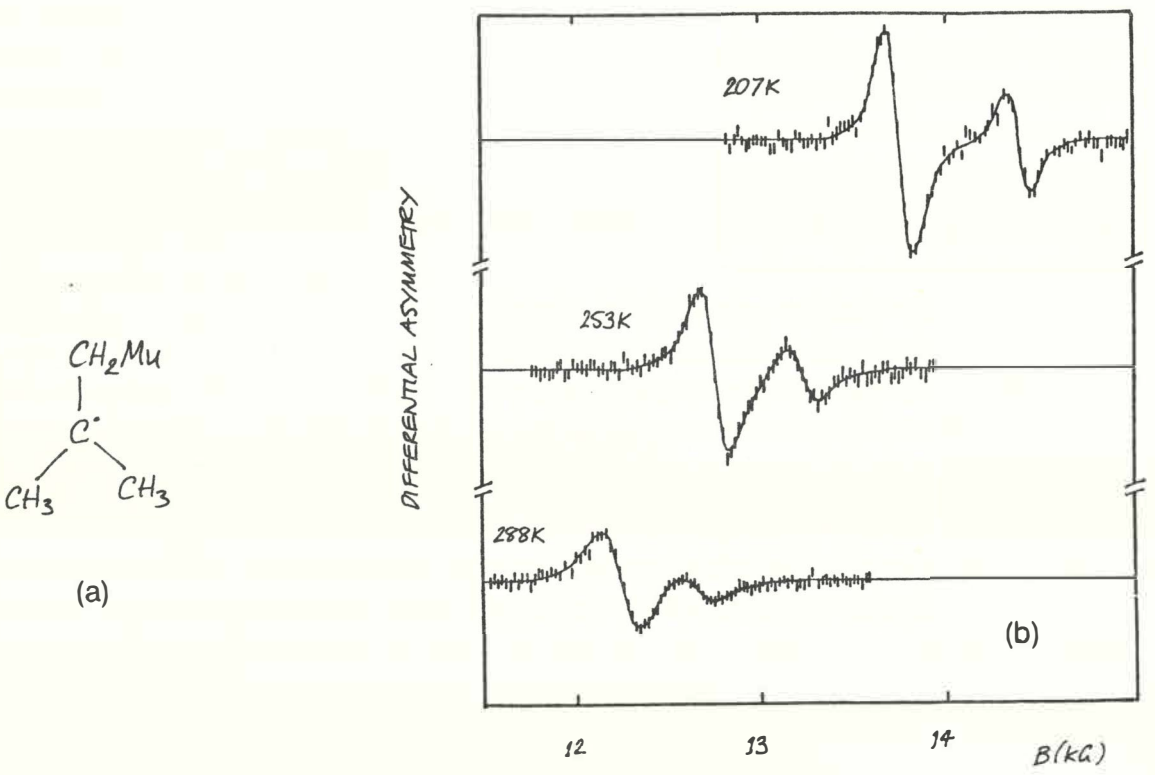

Figure 8. Structure of the t-butyl rdical (a) and its LCR spectra at various temperatures (b) /14/.

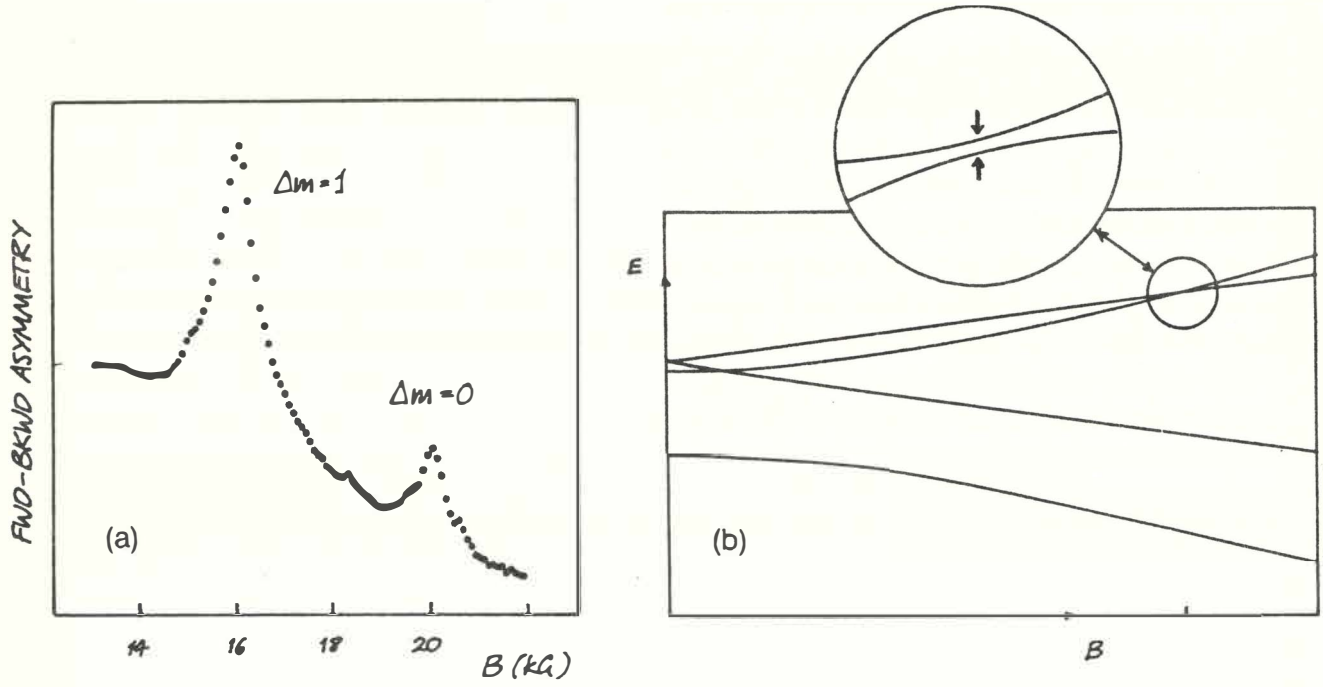

Figure 9. LCR spectra for $(CH_3)_2\dot{C}.CH_2Mu$ in solid isobutene (a), taken from/15/, and the simplified Breit-Rabi diagram drawn with a slightly anisotropic coupling to show the "pure muon" ($\Delta m = 1$) level crossing resonance (b).

Information is also available on molecular motion in these studies - in this case intramolecular reorientation. Unlike the ethyl radical, t-butyl shows a step change in A_μ at the melting point of the host (isobutene). The bonding to the trigonal carbon is thought to be slightly pyramidal, and the coupling between inversion at the radical centre and rotation of the peripheral methyl groups to be altered between the solid and liquid phases /15/.

The LCR spectrum of the same radical in the solid state is shown in Figure 9(a). It shows an additional feature which corresponds to a transition of the muon spin alone ($\Delta m = 1$). This resonance becomes allowed in the solid state because the intrinsic anisotropy of the couplings is preserved. The transverse component of the hyperfine field cannot be "tuned out" by the applied field at the level crossing depicted in Figure 9(b); the muon spin precesses about this transverse component and depolarises.

"Pure muon" resonances of this sort are potentially important in determining A_μ (not to mention its anisotropy) in the solid phase, where transverse field μSR spectra tend to be broadened (in the manner of powder spectra) beyond detection in non-crystalline media. That is, LCR alone can in principle provide full characterisation of radicals in the solid state.

11. ZERO POINT ENERGY

The above sections serve to illustrate the spectroscopic techniques and the type of data which is available. Some aspects of this data, notably the comparison of muon and proton hyperfine couplings, are interpreted below in terms of the different zero point energies of the two particles. This section serves to give a feeling for the energies involved.

A legitimate starting point for treating most problems in quantum chemistry and chemical physics is the adiabatic or Born-Oppenheimer approximation, namely the separation of nuclear and electronic wave-functions. A drastic further assumption is commonly adopted in considering ground-state molecular properties: this is to treat the nuclei as fixed at their equilibrium positions! This neglect of the Uncertainty Principle where nuclei are concerned rarely has detectable consequences for molecules containing heavy atoms. For these, a probability distribution characterising the nuclear nuclear positions is only necessary to describe excited vibrational states. For molecules containing light atoms, however, the nuclear positions are certainly not fully determinate; that is, the effects of zero point energy are are detectable.

To take the simplest example, the hydrogen molecule H_2 must dissociate slightly more readily than D_2, the difference in zero point energy between the protons and deuterons decreasing the "static" binding energy. Similar effects exist for all molecules containing H or D and are expected to be greatly enhanced when hydrogen is substituted by its light isotope Mu.

Figure 10 shows the "text-book" cases of particles confined within (a) a square well and (b) a harmonic potential, with energies for protons and muons calculated from the standard formulae. For the cubic box, the energy levels vary as the inverse of the particle mass

(equation 1) so that the ground state for a muon lies higher than that for a proton by a factor $m_p/m_\mu \simeq 9$! These levels vary as the inverse square of the confinement length L; for the fictitious 1Å box depicted, the fractional population of the first excited states, in thermal equilibrium at room temperature, would be small (10^{-3}) for the proton, and quite negligible (10^{-28}) for the muon.

$$E_n = n^2h/8mL^2 \text{ per dimension } (n = 1,2\ 3...) \quad (1)$$

A square well may be a reasonable approximation to some of the potentials encountered by muonium when trapped in interstitial cages in crystals. For the present case of muonium covalently bonded in molecules a harmonic oscillator potential, $V = \frac{1}{2}kx^2$, is generally more representative. For this, the energy levels are equally spaced and their mass dependence is weaker (equation 2). The ground state energy, as well as the vibrational frequencies, vary as $m^{-\frac{1}{2}}$ so that each level for the muon lies about 3 times higher than the corresponding level for the proton.

$$E = (n + \tfrac{1}{2})\hbar\omega = (n + \tfrac{1}{2})\hbar(k/m)^{\frac{1}{2}} \text{ per dimension } (n = 0,1\ 2...) \quad (2)$$

Roughly speaking, the muon ground state is on a level with the first excited state for the proton.

For the force constant used in Figure 10(b), the ground state rms displacement (equation 3) is 0.4Å for a muon and 0.23Å for a proton. The equilibrium populations at room temperature of the excited levels are negligible for both particles.

$$\langle x^2 \rangle^{\frac{1}{2}} = (mk)^{-\frac{1}{4}} (\hbar/2)^{\frac{1}{2}} \quad (3)$$

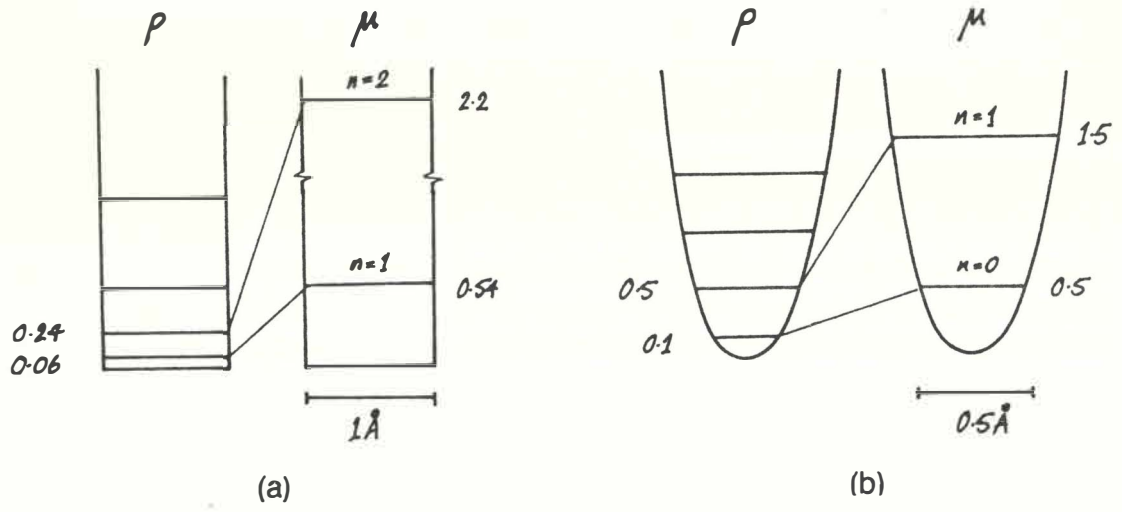

Figure 10. Energy levels for protons and muons confined within threedimensional square-well (a) and harmonic (b) potentials. Energy levels are calculated in eV for a cubic box of side 1Å in (a) and for a force constant of 25eV/Å^2 (400Nm^{-1} - this is about the value for a C-H bond) in (b). For conversion to other units, 1eV = 3.7x10^{-2}a.u = 96kj.mol^{-1} = 1.2 x10^{4}K.

Figure 11 shows the situation in a realistic potential or Morse curve for the C-X bond (X = H,Mu). Zero point energy makes the bond slightly weaker for X = Mu than for X = H; anharmonicty of the potential makes it on average slightly longer as well. Roduner and Reid /16/ estimate an extension of 0.06Å or 5% of the equilibrium separation.

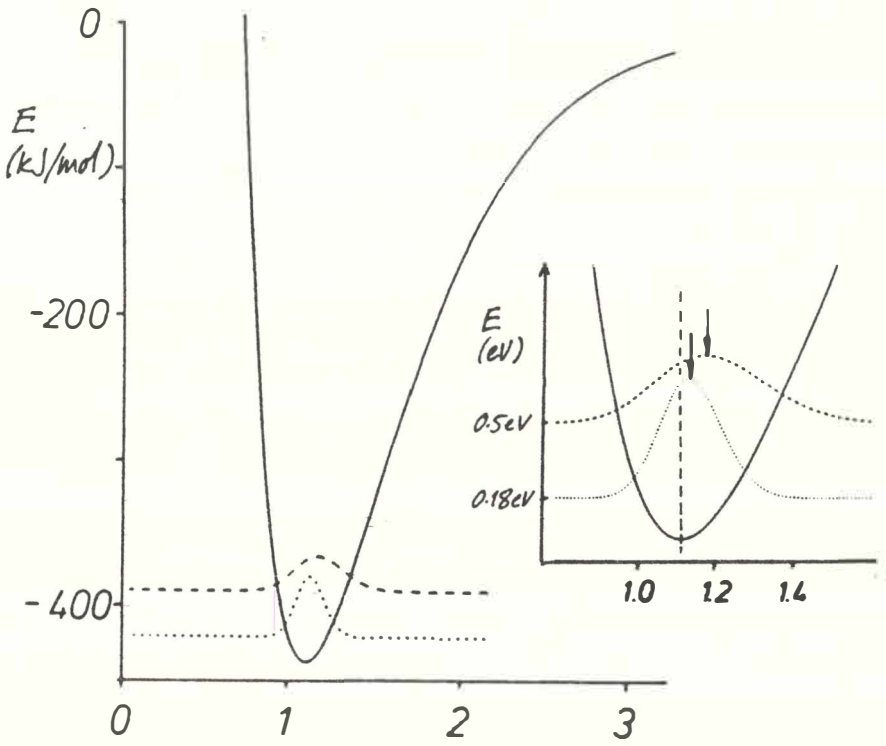

Figure 11. Morse curve for the C-X bond, zero point energies and bond length distributions (density distributions for the light nucleus if carbon is considered stationary) for X = H and X = Mu and, at right, the effective or dynamically averaged bond lengths (taken from /16/).

12. THE EFFECT ON CONFORMATION

The origin of the barrier to internal rotation in $\dot{C}H_2CH_2Mu$ can also be traced to the muon zero point energy. Claxton and Graham /17/ calculate the total energy of the molecule in the two extreme conformations, i.e. when the C-Mu bond adopts the eclipsed position (dihedral angle constrained to $\theta = 0$) and the staggered position ($\theta = 90°$). They also calculate the change in energy for small displacements of all nuclei about their equilibrium positions, i.e. the force constants for all bonds, and find that the molecule is slightly "stiffer" in the staggered conformation. Addition of the nuclear zero point energies then tips the energy balance in favour of the eclipsed conformation. The methylene protons even bend slightly out of the plane, towards the muon, as in Figure 12(a).

The case of internal rotational freedom admittedly presents a rather delicate energy balance, but such a pronounced isotope effect on molecular conformation is nonetheless remarkable.

13. THE RESIDUAL ISOTOPE EFFECT

Even when the orientational preference is allowed for, the spin density on the muon is nonetheless greater than on a proton in the same position, by about 20%. Referring to Figure 7(b), A'_μ does not become exactly equal to A_p even in the free rotation limit. This is best demonstrated by comparing the average coupling for the CH_2Mu group,

$$\overline{A} = 1/3(A'_\mu + 2A_p) = 79\text{MHz},$$

with the value 75 MHz for the CH_3 protons in the normal radical /8/.

14. DYNAMICAL AVERAGING OF THE HYPERFINE COUPLINGS

The origin of this difference is illustrated in Figure 12. As the C-X bond is stretched, spin-density an X increases rapidly as a non-linear function of C-X separation. In a qualitative (valence bond) description, this correspondsto an increasing mixture of (CH_2CH_2 + Mu(↑)) as opposed to C(↑)H_2CH_2Mu. In the limit, a muonium atom is withdrawn from the molecule - the reverse of its formation! The quantitative dependence has been calculated recently using ab initio (Unrestricted Hartree-Fock) methods by Claxton et al /18/.

The dynamically averaged spin density on X is therefore greater for X = Mu than for X = H, by virtue both of the (anharmonic) bond extension and the greater rms (harmonic) displacement of the lighter atom. The perpendicular normal modes also contribute to the net effect.

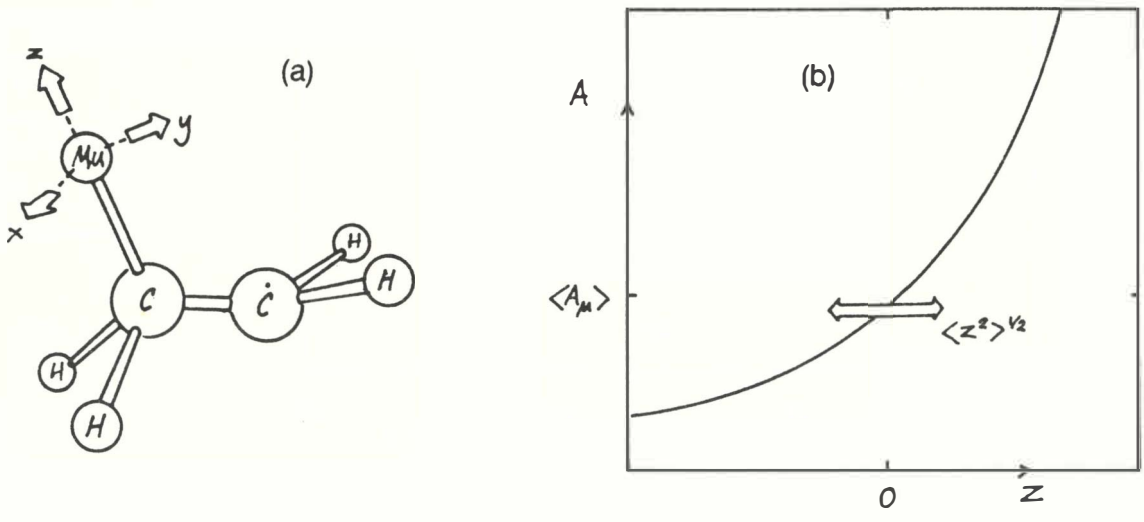

Figure 12. The eclipsed conformer of the ethyl radical (a) indicating the three normal modes of the muon and the variation of hyperfine coupling (b) with the stretch mode (sketched from /18/).

At risk of perpetuating a description which is no longer strictly necessary, this result may be taken as confirming the notion of enhanced hyperconjugation for the muon /19/. It would seem reasonable to retain qualitative "chemical" explanations and models as long as they provide reliable insight and correct productions!

15. DIAMAGNETIC MOLECULES

In most substances, some fraction of the muons implanted reach diamagnetic states. There is no signature of their identity in the μSR spectra, however, comparable with the hyperfine frequencies for paramagnetic species. These muons precess at close to their Larmor frequency. Chemical shifts are in general too small to resolve or measure. The diamagnetic fraction must represent muonium which is substituted in ionic or molecular species (or, where appropriate, in hydrogen bonds). LCR can in principle be used to identify the species, and the position adopted by the muon, in favourable cases.

The first such identification in a molecular species is illustrated in Figure 13. In this experiment, muons are implanted in ice, and the muon Zeeman energy is tuned to a quadrupole splitting on ^{17}O. The sample is enriched to about 50% in $H_2{}^{17}O$ for this purpose. In a diamagnetic species, the polarisation transfer can only be mediated by the muon-nuclear dipole-dipole interaction, which is effective only at short range. Detection of the resonance implies that the muon is chemically bonded to oxygen /20/: the species identified is the muonium-substituted or "ultralight" water molecule, HMuO. This is believed to be formed in the two stage process /21/:

$$H_2O + \mu^+ \rightarrow H_2MuO^+$$

$$H_2MuO^+ + H_2O \leftrightarrows HMuO + H_3O^+.$$

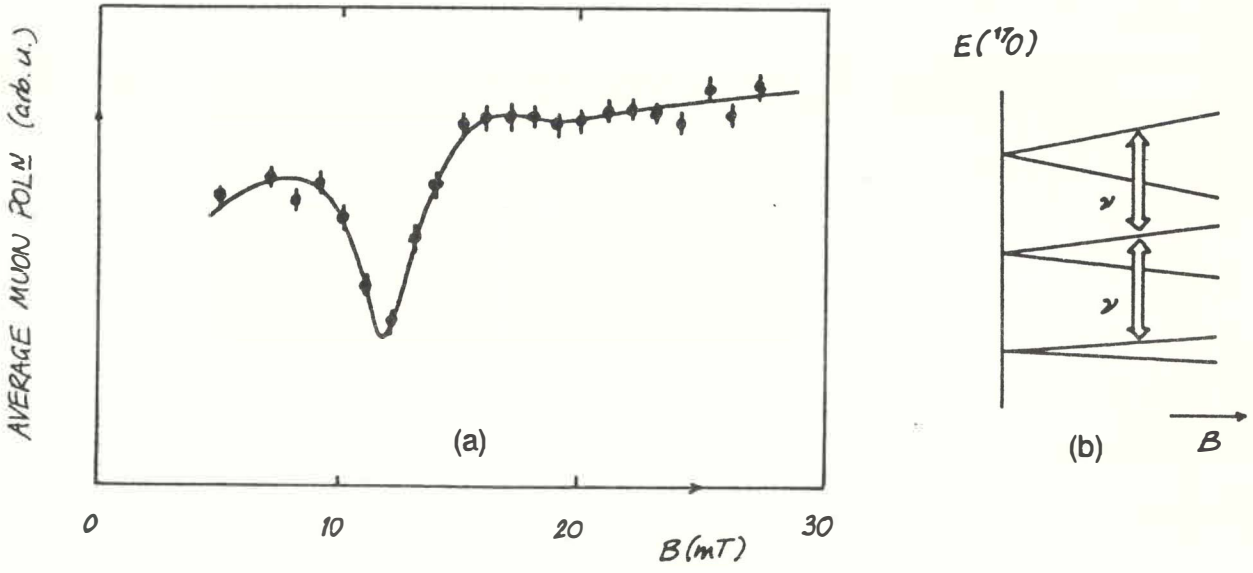

Figure 13. LCR spectrum for $HMu^{17}O$ in ice (a) and the (approximately equal) quadrupole splittings involved (b) (taken from /22/).

16. THE QUADRUPOLE ISOTOPE EFFECT

The quadrupole splittings ν on ^{17}O in ordinary ice are known from the conventional NQR literature. These can be used to predict the position of the resonance:

$$B_{res} = 2\pi\nu/(\gamma_\mu - \gamma_O).$$

The resonance is found at a field which is 5-10% lower than this prediction, implying a correspondingly smaller value for the quadrupole coupling in the muonium substituted molecule. This is the first such measurement of a quadrupole isotope effect by μSR.

It is interesting that the electric field gradient at the oxygen nuclei already decreases by some 30% between vapour and ice - an unusually large change which is attributed to the effects of hydrogen bonding in the condensed phase. The further reduction on going from H_2O to HMuO in ice may be understood in terms of an enhancement of these effects in the vicinity of a muonium bond, namely a greater polarisation of the substituted (and neighbouring) molecules, more nearly tetrahedral bonding and therefore greater symmetry of the charge distribution surrounding the oxygen nuclei involved. This is explained in terms of the anharmonicity of the proton (muon) potential in a hydrogen (muonium) bond, together with the larger zero point energy of the lighter particle. The mechanism is illustrated in Figure 14.

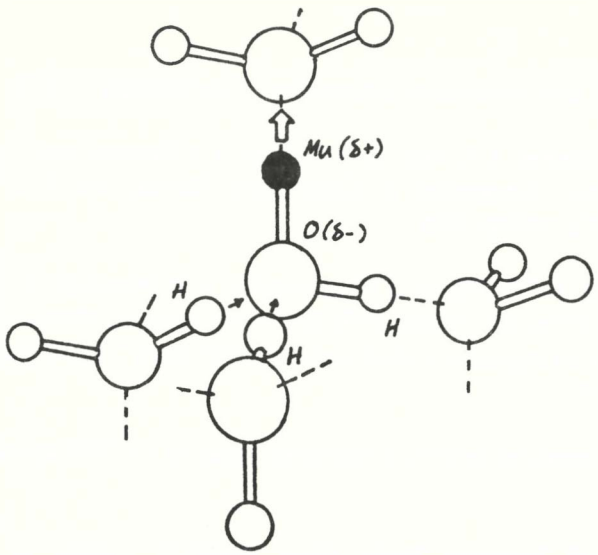

Figure 14. Possible effects of muonium substitution on bond lengths and polarisation in ice /22/.

This intuitive picture remains to be confirmed by quantum-chemical calculations. Since the available (e.g. ab initio) methods are able to compute the distribution of charge density more reliably than they are that of spin density, measurements of quadrupole isotope effects may prove to be a valuable source of data with which to check these methods, and perhaps capable of a more certain interpretation than the hyperfine isotope effect in radicals of the muon and proton dynamics.

17. FUTURE POSSIBILITIES

The possibility of measuring muon-proton dynamic isotope effects in other molecular properties should not be overlooked. Dipole moment is an obvious candidate.

The various contributions to these effects would be easier to unravel if the normal modes associated with the muon motion could be isolated with laser spectroscopy. This may prove

possible: the characterisic frequency of the stretching mode of C-X or O-X bonds should be greater for X = Mu than for X = H by a factor of approximately $(m_p/m_\mu)^{1/2} \simeq 3$, which is sufficient to detach these modes from the rest of the vibrational spectrum. A form of trigger detection could be envisaged, in which a particular μSR or LCR transition is monitored whilst the laser frequency is swept: a resonant loss of signal would indicate a vibrational excitation and allow its characteristic frequency to be determined.

REFERENCES

1. D C Walker, "Muon and muonium chemistry" Cambridge (1983)

2. D G Fleming, D M Garner, L C Vaz, D C Walker, J H Brewer and K M Crowe, "Positron and Muonium Chemistry" Advances in Chemistry Series, ed H J Ache (Am Chem Soc, Washington DC) **175** (1979) 279

3. E Roduner, W Strub, P Burkhard, J Hochmann, P W Percival, H Fischer, M Ramos and B C Webster, "Chem Phys **67** (1982) 275 (for more recent references, see also E Roduner: "The positive muon as a probe in free radical chemistry", Springer Verlag Lecture Notes in Chemistry **49** (1988)

4. M C R Symons, "Chemical and biochemical aspects of ESR spectroscopy" Van Nostrand Reinhold (1978)

5. S F J Cox and M C R Symons, Radiat Phys Chem **27** (1986) 53

6. Estimated by E Roduner: private communication (1990)

7. E Roduner and D M Garner, Hyp Int **32** (1986) 733

8. P W Percival, J-C Brodovitch, S-K Leung, D Yu, R F Kiefl, D M Garner, D J Arseneau, D G Fleming, A Gonzalez, J R Kempton, M Senba, K Venkataswaran and S F J Cox, Chem Phys Lett **163** (1989) 241

9. A Abragam, CR Acad Sci (Paris) **299** (1984) 95

10. R F Kiefl, S R Kreitzman, M Celio, R Keitel, G M Luke, J H Brewer, D R Noakes, P W Percival, T Matsuzaki and K Nishiyama, Phys Rev **A34** (1986) 681

11. M Heming, E Roduner, B D Patterson, W Odermatt, J Schneider, H Baumeler, H Keller and I M Savic, Chem Phys Lett **128** (1986) 100

12. M J Ramos, D McKenna, B C Webster and E Roduner, J Chem Soc Faraday Trans I **80** (1984) 255 and 267

13. P W Percival, J-C Brodovitch, S-K Leung, D Yu, R F Kiefl, D M Garner, G M Luke, K Venkataswaran and S F J Cox, "Intramolecular motion in organic radicals", IOP Short Meetings Series (IOP Bristol) **22** (1989) 99

14. P W Percival, R F Kiefl, S R Kreitzman, D M Garner, S F J Cox, G M Luke, J H Brewer, K Nishiyama and K Venkataswaran, Chem Phys Lett **135** (1987) 465

15. P W Percival, J-C Brodovitch, S-K Leung, D Yu, R F Kiefl, G M Luke, K Venkataswaran and S F J Cox, Chem Phys **127** (1988) 137

16. E Roduner and I D Reid, Israel J Chem **29** (1989) 3

17. T A Claxton and A M Graham, J Chem Soc Faraday Trans I **83** (1988) 2307

18. T A Claxton, S F J Cox, A M Graham, Dj Maric, P F Meier and S Vogel, Hyp Int and Proc μSR 90 (at press)

19. M C R Symons, Hyp Int **17-19** (1984) 771, and S F J Cox, T A Claxton and M C R Symons. Radiat Phys Chem **28** (1986) 107

20. S F J Cox, G H Eaton, J E Magraw and C A Scott, Chem Phys Lett **160** (1989) 85

21. P W Percival, Radiochimica Acta **26** (1979) 1

22. S F J Cox, J A S Smith and M C R Symons, Hyp Int and Proc μSR90 (at press)